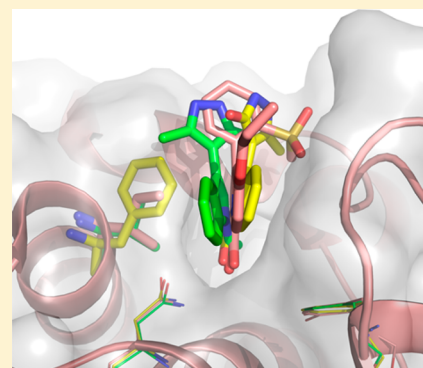


The “Gatekeeper” Residue Influences the Mode of Binding of Acetyl Indoles to Bromodomains

Andrea Unzue,[†] Hongtao Zhao,[‡] Graziano Lolli,[‡] Jing Dong,[‡] Jian Zhu,[‡] Melanie Zechner,[†] Aymeric Dolbois,[†] Amedeo Caflisch,^{*,‡} and Cristina Nevado^{*,†}[†]Department of Chemistry and [‡]Department of Biochemistry, University of Zürich, Winterthurerstrasse 190, CH-8057 Zürich, Switzerland

Supporting Information

ABSTRACT: Small-molecule hits for the bromodomains of CREBBP and BAZ2B have been identified by scaffold hopping followed by docking of a set of ~200 compounds containing the acetyl indole scaffold. Chemical synthesis of nearly 30 derivatives has resulted in ligands of representatives of three subfamilies of human bromodomains with favorable ligand efficiency. The X-ray crystal structures of three different bromodomains (CREBBP, BAZ2B, and BRPF1b) in complex with acetyl indole derivatives reveal the influence of the gatekeeper residue on the orientation of small-molecule ligands in the acetyl lysine binding site.



INTRODUCTION

Acetylation of lysine residues is an important post-translational modification of histone proteins that contributes to the regulation of chromatin structure and transcription.^{1,2} Bromodomains are protein modules with four-helix bundle topology that specifically recognize (“read”) acetylated lysine residues, as well as butyryllysine and crotonyllysine,³ and are considered protein targets of interest for the development of chemical probes and clinical tools for the treatment of cancer, inflammation, and other diseases.^{4–8}

The BET (bromodomain and extra terminal) subfamily (BRD2/3/4/T) has been widely addressed, and as a consequence, several potent and selective inhibitors have been developed, some of which are currently undergoing clinical trials for the treatment of NUT midline carcinoma (NMC), solid tumors, leukemia, lymphoma, hematological malignancies, atherosclerosis, and type II diabetes.^{7,9,10} In contrast, the specific function and potential pharmacological relevance of other bromodomains, including CREB binding protein (CREBBP), E1A binding protein p300 (EP300), BRD7/9, and bromodomain adjacent to zinc finger domain (BAZ2B), are much less understood, and thus, small-molecule inhibitors will be valuable tools for unraveling their biological roles.

The bromodomains of EP300 and CREBBP, which belong to the same subfamily and share 96% sequence identity,¹¹ play important roles in DNA replication and repair, cell growth and cell cycle regulation, and genomic stability.^{12,13} As an example, EP300 and CREBBP are able to acetylate p53 on its K382 residue through the histone acetyl transferase (HAT) domain upon extracellular stress or DNA damage, and they are also

known to specifically bind to acetylated p53 via their bromodomain module.¹⁴ As a consequence, changes in the p53-dependent activation of target genes result in cell cycle arrest, senescence, or apoptosis.^{15–17} On one hand, chromosome translocations resulting in gene fusions containing CREBBP or EP300 have been linked to leukemias and lymphomas.^{18,19} On the other hand, CREBBP and EP300 are mutated in solid tumors and B-cell lymphoma, suggesting they possess a tumor-suppressing role.^{13,20} Thus, because both oncogene or tumor suppressor roles have been reported for CREBBP and EP300,^{18,21} the development of chemical probes will be instrumental for the analysis of their biological function(s).

The bromodomains of BRD7 and BRD9 belong to the same subfamily and share 72% sequence identity.²² Both BRD7 and BRD9 are part of the SWI/SNF (SWItch/Sucrose Non-Fermentable) chromatin remodelling complex, which plays a key role in the regulation of gene expression.^{23–25} Recent reports have linked BRD9 to oncology, including non-small cell lung²⁶ and cervical cancer.²⁷ Its paralogue, BRD7, is frequently downregulated in cancer^{28–30} and is able to regulate the tumor suppressor protein p53.^{31–33} The bromodomain of BRPF1b (bromodomain-PHD finger protein 1b) belongs to the same subfamily as BRD7 and BRD9. Despite the function of the BRPF1b bromodomain not being yet fully understood, the availability of BRPF1b ligands might help in the elucidation of its role.^{34–36}

Received: November 10, 2015

Published: March 16, 2016

BAZ2B is another bromodomain-containing protein whose role in physiology and disease is not clear. Biophysical screening of a library of 1300 fragments resulted in the identification of 10 small molecules that bind in the micromolar range to BAZ2B.³⁷ Recently, the first submicromolar selective CREBBP,^{11,38,39} BAZ2B,^{40,41} and BRD7/9^{22,42,43} inhibitors have been reported.

Here we present the result of a combined scaffold hopping and docking approach that has permitted the discovery of acetyl indoles as ligands of the bromodomains of CREBBP, BAZ2B, BRPF1b, and/or BRD9, which belong to three different subfamilies that lie outside of the BET bromodomain subfamily. A comparative analysis of four crystal structures of bromodomain/acetyl indole complexes shows the importance of the so-called gatekeeper residue with respect to the binding mode of the ligand.

RESULTS AND DISCUSSION

In Silico Screening by Scaffold Hopping and Docking.

In the past few years, our groups have successfully identified several low micromolar to nanomolar kinase^{44–47} and bromodomain^{39,48,49} inhibitors by high-throughput virtual screening campaigns. In this work, we decided to dock a small subset of compounds containing a moiety identified by scaffold hopping (see [Experimental Section](#)). First, the ZINC all-now library was decomposed into approximately 600000 fragments retaining key functional groups. These fragments were queried by the indolizine fragment **A**, which is present in the potent BAZ2B ligand GSK2801 (**1a**)⁴¹ and more recently has been identified in BRD7 and BRD9 ligands.²² (Capital letters are used to label generic chemical blueprints. **1a–i** correspond to commercially available compounds. **1–50** represent the synthetic intermediates and self-made products.) The acetyl indole **B** was identified as the top-ranking fragment with an activity-oriented fingerprint similarity of 0.975 with respect to **A**. The high degree of similarity is due to almost identical geometry and connecting vectors in fragments **A** and **B** ([Figure 1](#)).

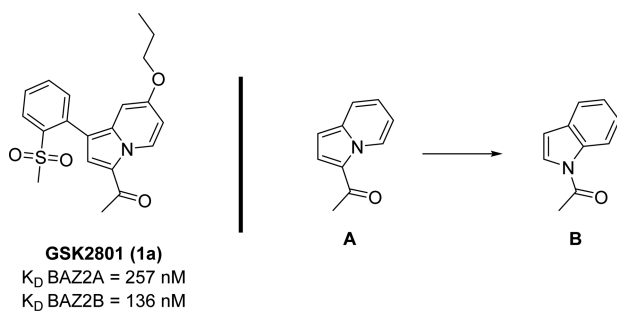


Figure 1. GSK2801 (**1a**), a nanomolar chemical probe for BAZ2A and BAZ2B bromodomains.^{22,41} Core fragment hopping by activity-oriented fingerprint using fragment **A** as the query molecule. **A** and **B** represent generic chemical blueprints.

In a second step, we retrieved ~200 commercially available compounds containing fragment **B**. As in our previous fragment-based virtual screening approach,^{46,48,49} the retrieved compounds were docked into crystal structures of the targets, namely, the bromodomains of CREBBP [Protein Data Bank (PDB) entry 4A9K] and BAZ2B (PDB entry 3Q2F). An in-house-developed program for automatic docking was used.^{48,50–52} The docking poses were subsequently rescored

by a transferable scoring function (see [Experimental Section](#)).^{45,50–54} Finally, 14 molecules were selected for experimental validation by means of a competition binding assay.^{55,56} At a concentration of 50 μ M, seven compounds showed significant competition [i.e., a percentage of residual binding of CREBBP to the acetylated histone peptide of <70% with respect to the DMSO control ([Figure 2](#))], which corresponds to a hit rate of 50% for the *in silico* screening approach based on scaffold hopping and docking. The most active compound, **1b**, exhibits an equilibrium dissociation constant (K_d) of 20 μ M for CREBBP. Using the same threshold of 70% as for CREBBP, the hit rate for BAZ2B was 29% ([Figure 2](#)). Interestingly, at a concentration of 50 μ M, only compound **1g** shows a significantly higher affinity for BAZ2B than for CREBBP.

Binding Mode of Compound 1b: Validation by X-ray Protein Crystallography. The opposite selectivity toward CREBBP and BAZ2B observed for compounds **1b** and **1g** ([Figure 2](#)) prompted us to study their binding mode. While we could not determine the structure with compound **1g**, the crystal structure of CREBBP in complex with compound **1b** was determined at 2.0 Å resolution ([Figure 3](#), green, PDB entry 4TS8), which revealed an overall binding mode essentially identical to the docked pose of compound **1b** ([Figure 3](#), blue). The binding of compound **1b** in CREBBP is characterized by a lipophilic sandwich of its bicyclic core between residues Phe1111, Val1174, and Ala1164 on one side and Val1115, Leu1120, and Ile1122 on the other side of the binding pocket. The carbonyl oxygen of the acetyl indole acts as the acetylated lysine mimic and is engaged in hydrogen bonding interactions with the side chains of the conserved Asn1168 (BC loop) and Tyr1125 (ZA loop), where the latter is bridged by a water molecule. Another four water molecules present at the bottom of the pocket are conserved. In addition, there is a water molecule bridging the dihydro-pyrazole ring and the guanidinium group of Arg1173 ([Figure 3](#)).

Assessing the Affinity Difference between Indolizine and Indole Ligands. Compound **1a** is reported to be a potent ligand for the BAZ2B bromodomain with a K_d of 136 nM.⁴¹ To study the influence on the binding affinity of the position of the nitrogen atom in our hit compound **1b**, we decided to synthesize the indole analogue of indolizine **1a**. Commercially available 1*H*-indol-5-ol (**1**) was transformed into compound **3** via alkylation of the phenol moiety with 1-iodopropane, followed by introduction of an *N*-benzenesulfonyl group and bromination at C3 in the presence of molecular bromine ([Scheme 1](#)). Bromo indole **3** was then coupled to [2-(methylsulfonyl)phenyl]boronic acid, affording compound **4** in moderate yield. Removal of the sulfonyl group under basic conditions preceded the incorporation of the acetyl group to give the indole analogue of compound **1a** (**5**).

Interestingly, a 24-fold reduction in binding affinity toward BAZ2B was observed for acetyl indole **5** with respect to **1a** [IC_{50} values of 8.55 and 0.36 μ M, respectively, determined by AlphaScreen (see the [Supporting Information](#))], which indicates that the position of the nitrogen atom in the double-ring system is crucial.

Synthesis. We decided to focus our derivatization campaign on compounds **1b** and **1g** as ligands. Compound **1b** was selected because of its ligand efficiency for CREBBP (0.34 kcal/mol per heavy atom) and the availability of the crystal structure ([Figure 3](#)), while compound **1g** was chosen because of its selectivity toward BAZ2B ([Figure 2](#)).

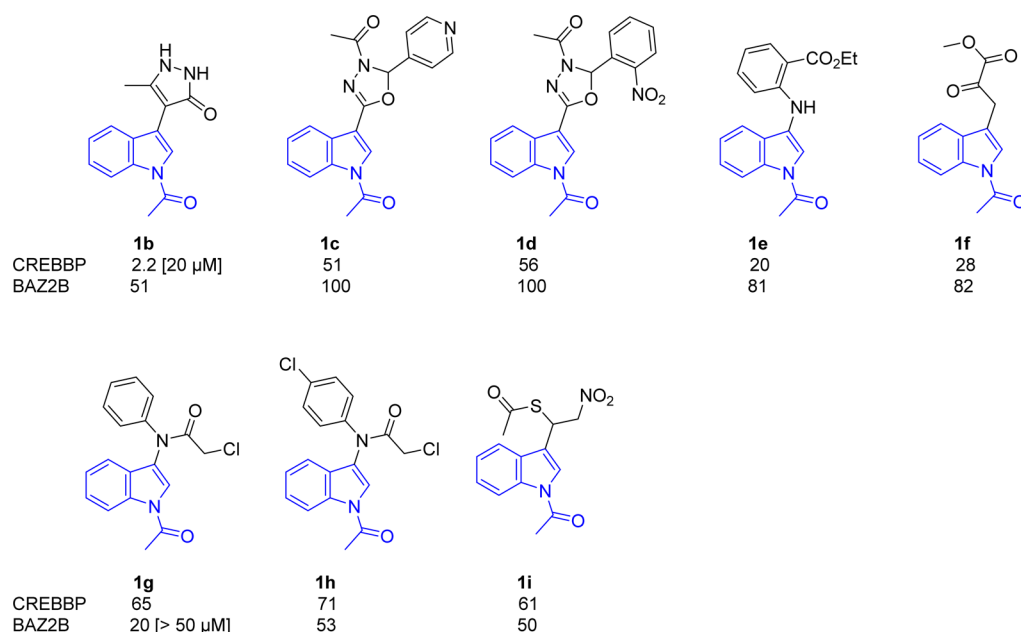


Figure 2. Binding affinity and two-dimensional structures of acetyl indole derivatives **1b–i** identified by core fragment hopping and docking. The values are a percentage of residual binding of the CREBBP or BAZ2B bromodomain to an acetylated histone peptide at a compound concentration of 50 μ M with respect to the DMSO control. Thus, lower percentages indicate higher affinities of the compound. Values in brackets are equilibrium dissociation constants (K_d) determined by two independent dose–response measurements of 11 doses each. Compounds **1c**, **1d**, and **1i** were measured as a racemic mixture. All values were determined by the BROMOscan competition binding assay.^{55,56}

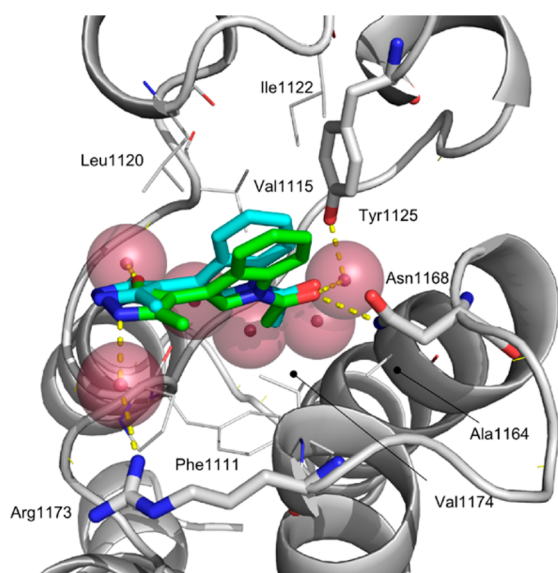
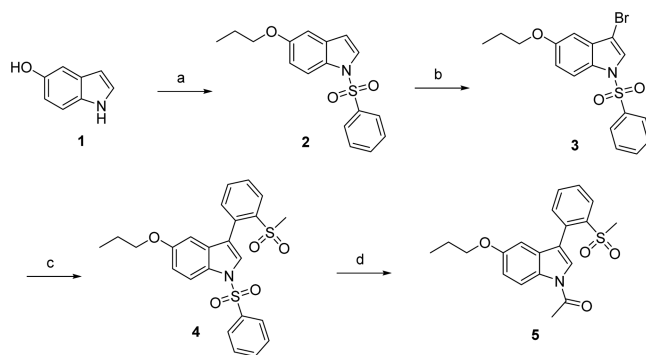


Figure 3. Crystal structure (green) and docked pose (blue) of the CREBBP bromodomain (gray) in complex with compound **1b** (PDB entry 4T58). The conserved Tyr1125 and Asn1168 residues, together with Arg1173 (a characteristic residue for the CREBBP bromodomain),^{11,38,39,49} are shown as sticks. Hydrogen bonds are shown as yellow dashed lines, and the crystallographic water molecules are represented by red spheres.

Synthesis of Compound 1b and Its Derivatives. The synthesis of CREBBP hit **1b** is shown in Scheme 2. The carboxylic acid of commercially available 2-(1H-indol-3-yl)-acetic acid (**6**) was transformed into the corresponding methyl ester. Acetylation of the N atom afforded indole **7**. Deprotonation of **7** in the presence of *in situ*-generated lithium diisopropylamide (LDA) followed by reaction with acetic anhydride or 4-methoxyphenylacetic anhydride delivered

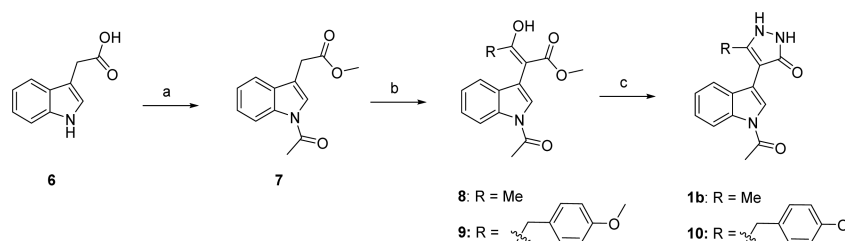
Scheme 1^a



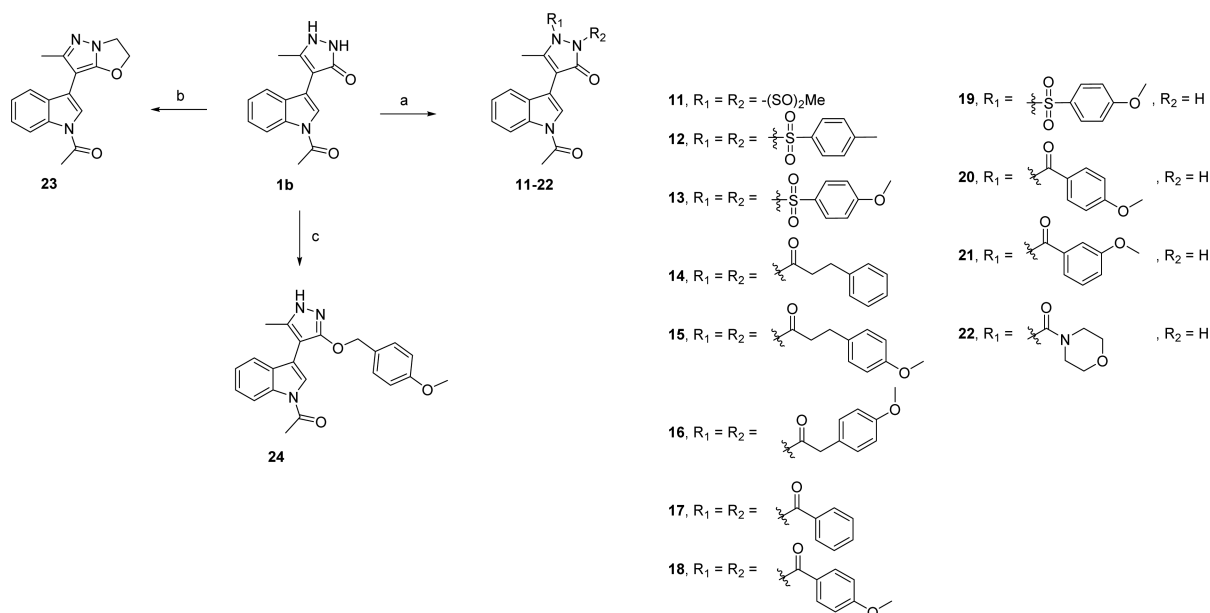
^aReagents and reaction conditions: (a) (i) 1-iodopropane, K_2CO_3 , acetone, reflux, 72 h, 84%; (ii) benzenesulfonyl chloride, TBAB, 50% NaOH, H_2O , toluene, 0–25 $^{\circ}C$, 69 h, 97%; (b) Br_2 , DMF, 25 $^{\circ}C$, 7 h, 47%; (c) [2-(methylsulfonyl)phenyl]boronic acid, 1 M $NaHCO_3$, $Pd(PPh_3)_4$, DME, 25–85 $^{\circ}C$, 15 min, 33%; (d) (i) 2 M NaOH, MeOH, 85 $^{\circ}C$, 5 h, 69%; (ii) AcCl, NaOH, TBAHS, DCM, 25 $^{\circ}C$, 13 h, 63%. Abbreviations: TBAB, tetra-*n*-butylammonium bromide; DMF, dimethylformamide; DME, 1,2-dimethoxyethane; TBAHS, tetrabutylammonium hydrogen sulfate.

intermediate **8** or **9**, respectively. Cyclization in the presence of hydrazine hydrate afforded hit compound **1b** and derivative **10** in moderate yields (Scheme 2).

Hit compound **1b** was then reacted with a variety of acid and sulfonyl chlorides, affording disubstituted (**11–18**) as well as monosubstituted dihydro-pyrazole derivatives (**19–22**) as indicated in Scheme 3. Two more derivatives were prepared: upon condensation of 1,2-dibromoethane with compound **1b** in the presence of K_2CO_3 , derivative **23** was obtained. The reaction of **1b** with *p*-methoxybenzyl bromide in the presence of NaH afforded O-alkylated product **24** (Scheme 3).

Scheme 2^{4a}

^{4a}Reagents and reaction conditions: (a) (i) MeOH, H₂SO₄, 25 °C, 1 h, 94%; (ii) Ac₂O, DMAP, Et₃N, THF, 25 °C, 17 h, 90%; (b) (iPr)₂NH, *n*-BuLi, THF, -75 °C, 1 h, then, acetic anhydride or 4-methoxyphenylacetic anhydride, -78 °C, 2–4 h; (c) hydrazine hydrate, camphoric acid, EtOH, toluene, 93 °C, 30 min–1 h, 29–51% over two steps. Abbreviation: DMAP, 4-dimethylaminopyridine.

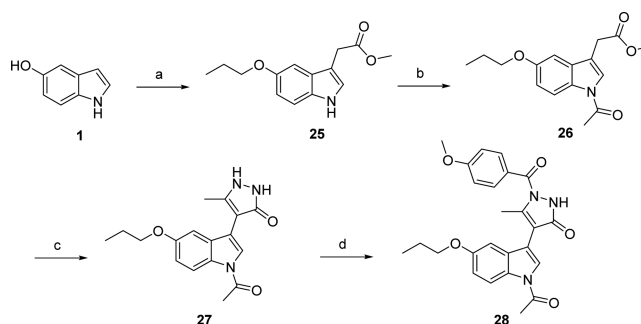
Scheme 3^{4a}

^{4a}Reagents and reaction conditions: (a) R-Cl, Et₃N, DCM, 0–25 °C, 5–12 h, 24–89%; (b) 1,2-dibromoethane, K₂CO₃, DMF, 80 °C, 7 h, 41%; (c) PMB-Br, NaH, TBAI, DMF, 0–25 °C, 1.5 h, 23%. Abbreviations: PMB, 4-methoxybenzyl ether; TBAI, tetrabutylammonium iodide.

Finally, we decided to incorporate the propoxy group at position 5 of the indole, for which a similar protocol was applied to 1*H*-indol-5-ol (**1**), delivering the final products **27** and **28** (Scheme 4).

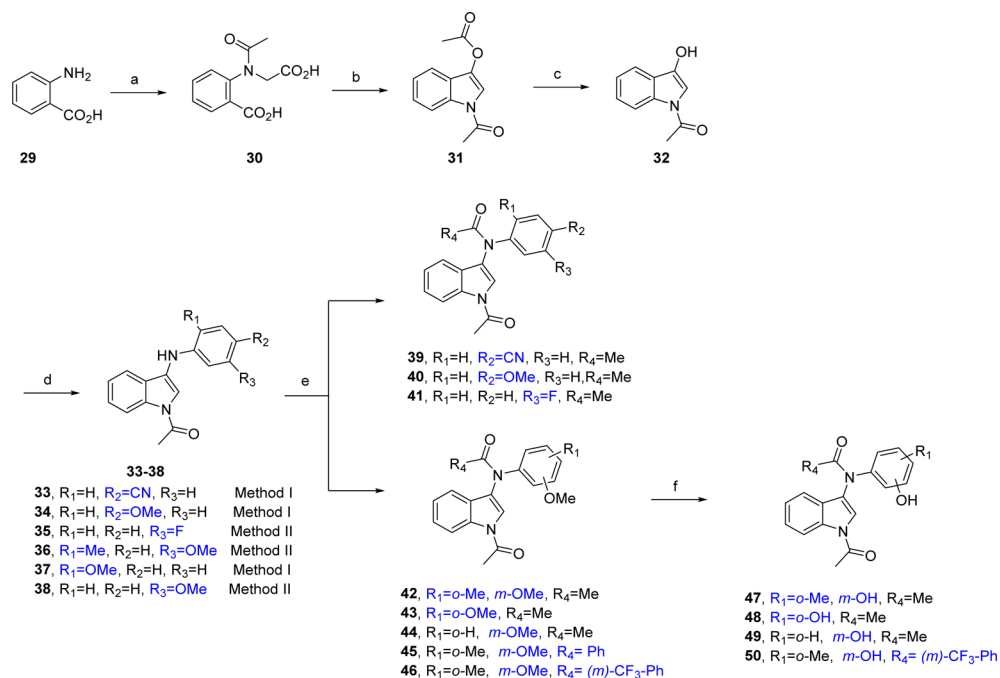
Synthesis of Derivatives of Compound 1g. The common intermediate for the synthesis of derivatives of ligand **1g** was obtained from the commercially available non-natural amino acid **29** in four steps with a 20% overall yield (Scheme 5). Condensation of intermediate **32** with diverse commercially available anilines afforded acetyl indole intermediates **33–38**, which were then acylated in the presence of diverse acid chlorides, affording compounds **39–46**. Four additional derivatives were prepared by cleaving the methoxy substituent in the presence of BBr₃ to produce phenol derivatives **47–50** (Scheme 5).

Biophysical Characterization. *Compound 1b and Its Derivatives.* Compound **1b** was screened against a panel of 10 different bromodomains using a thermal shift assay (Table 1 and Table S2 in the Supporting Information). This initial screening revealed BRD9 bromodomain as a potential off target for compound **1b** with a shift in the melting temperature of 1.3 °C, which translated into a K_D of 5.3 μM, as measured by a competition binding assay,^{55,56} and a ligand efficiency (LE)

Scheme 4^{4a}

^{4a}Reagents and reaction conditions: (a) (i) 1-iodopropane, K₂CO₃, acetone, reflux, 72 h, 84%; (ii) (COCl)₂, Et₂O, 0 °C, then NaOMe in MeOH, -78 °C, 3 h; (iii) Pd/C, NaH₂PO₂, dioxane, H₂O, 25 °C, 12 h, 88% over two steps; (b) Ac₂O, DMAP, Et₃N, THF, 25 °C, 12 h, 42%; (c) (i) (iPr)₂NH, *n*-BuLi, THF, -78 °C, 1 h, then, acetic anhydride, -78 °C, 4 h; (ii) hydrazine hydrate, camphoric acid, EtOH, toluene, reflux, 4 h, 18%; (d) 4-methoxybenzoyl chloride, Et₃N, DCM, 0–25 °C, 12 h, 19%.

value of 0.38 kcal/mol per heavy atom. This result is in line with the recent work of Brennan and co-workers, who

Scheme 5^a

^aReagents and reaction conditions: (a) (i) chloroacetic acid, K₂CO₃, H₂O, 90 °C, 16 h; (ii) Ac₂O, 25 °C, 30 min, then 37% HCl for 12 h, 33% over two steps; (b) Ac₂O, Et₃N, reflux, 30 min, 89%; (c) Na₂SO₃, reflux, 2 h, 83%; (d) method I: aniline, AcOH, reflux, 1–8 h, 26–56%; method II: aniline, pTSA, toluene, reflux, 2.5–4 h, 50–52%; (e) for MeCOCl, toluene, reflux, 12 h, 36–78%; if R₄ = aryl, R₄COCl, toluene, Et₃N, DMAP, 100 °C, 1 h, 13–21%; (f) BBr₃, DCM, 0–25 °C, 1–12 h, 47–84%. Abbreviation: pTSA, *p*-toluenesulfonic acid.

developed BRD7 and BRD9 nanomolar potent indolizine derivatives starting from the BAZ2B inhibitor **1a**.²² Importantly, no activity of compound **1b** was observed for the tested BET family members, BRD4(1) and BRD4(2) (see the Supporting Information).

Because of the involvement of the acetyl group of compound **1b** in hydrogen bonds with the conserved Asn1168 and Tyr1125 residues of CREBBP (Figure 3), we decided to maintain this moiety and introduce the main modifications at the dihydro-pyrazole ring to gain affinity for CREBBP.

On the outset, we decided to modulate the interactions of the solvent-exposed NH groups of the dihydro-pyrazole ring. To do so, mono- and disubstituted amide and sulfonamides that could establish new interactions with the surrounding amino acid residues, including the characteristic Leu1109 and Arg1173 residues in the CREBBP bromodomain and His42 and Phe44 in BRD9, were incorporated [compounds **11**–**22** (Table 1)]. The presence of methyl-substituted sulfonamides in compound **11** provided a K_D of 6.6 μM in CREBBP, which is a 3-fold binding affinity improvement with respect to the hit compound **1b** and corresponds to a LE value of 0.26 kcal/mol per heavy atom.

In an effort to form π -stacking interactions with Arg1173 in CREBBP,^{11,38} and residues Phe43 and Phe44 in BRD9, aromatic substituents, some of them electron-rich, were incorporated (compounds **14**–**18**, **20**, and **21**). Compound **14** yielded the most active ligand toward BRD9 with a K_D of 3.5 μM. Interestingly, the presence of a *p*-methoxybenzoate substituent in compound **20** resulted in a 2-fold improvement of binding affinity with a thermal shift of 3.3 °C in CREBBP and a K_D of 9.3 μM. At the same time, compound **20** retained the activity toward BRD9 with a thermal shift of 5.1 °C and a K_D of 6.3 μM. The presence of a morpholine ring at the same

position (derivative **22**) could only slightly improve the binding affinity for CREBBP with a K_D of 12 μM.

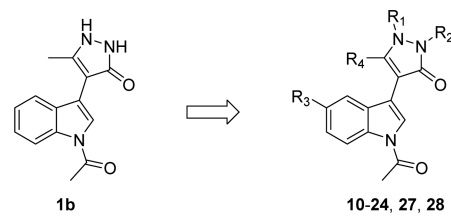
A dihydro-pyrazolo-oxazole ring was installed (compound **23**), which allowed us to revert the hydrogen bond donor capacity of the dihydro-pyrazole ring bearing two NH groups to a hydrogen bond acceptor-fused ring. Remarkably, compound **23** showed a K_D of 6.2 μM in CREBBP and retained the LE of the initial hit (0.34 kcal/mol per heavy atom), which makes it an attractive lead for further optimization. On the other hand, compound **24** exhibited a drop in the thermal shift, probably due to steric clashes of the *p*-methoxybenzyl group.

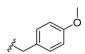
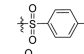
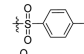
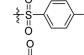
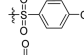
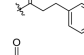
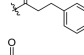
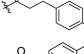
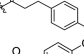
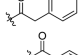
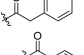
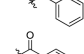
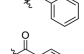
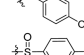
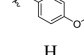
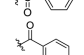
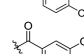
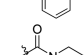
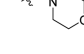
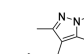
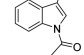
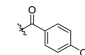
We then aimed to establish new interactions with the hydrophobic residues located on top of the binding site, Ile1122 and Leu1120 in CREBBP and Ala54 and Ile53 in BRD9, by substitution of the indole moiety at position 5 with a propoxy group (Table 1, compounds **27** and **28**), a modification that has proven to be successful in our previous work and in compound **1a**.^{39,41} Unfortunately, the presence of the propoxy substituent retained an activity of ~10 μM.

Importantly, with the exception of compounds **14** and **23**, all derivatives displayed ΔT_m values of <0.6 °C for BRD4(1), one of the most promiscuous bromodomains.^{11,38,57}

Compound 1g and Its Derivatives. Intrigued by the selectivity difference observed in the hit compound **1g** toward BAZ2B (Figure 2), we decided to examine its binding mode more closely. As we could not obtain crystals of the complex of compound **1g** with BAZ2B, several analogues were synthesized (Table 2), aiming not only to obtain a crystal structure of the complex but also to improve the binding affinity for BAZ2B. The chloroacetamide moiety was replaced by metabolically more stable amides in all derivatives to avoid covalent binding to the protein.

Table 1. Evaluation of Compounds 10–24, 27, and 28 Derived from 1b



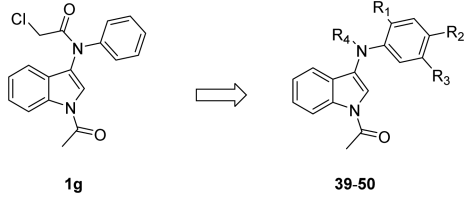
Cmpd	R ₁	R ₂	R ₃	R ₄	ΔT_m (°C) ^[a]				K_d (μM) ^[b]	
					CBP	EP300	BRD9	BRD4(1)	CBP	BRD9
1b	H	H	H	Me	0.3 (0.1)	0.4 (0.1)	1.3 (0.1)	-0.1 (0.1)	20.0	5.3
10	H	H	H		-0.1 (0.2)	-0.6 (0.2)	-0.8 (0.7)	-0.9 (0.4)	-	-
11	-SO ₂ Me	-SO ₂ Me	H	Me	2.2 (0.2)	2.7 (0.1)	1.0 (0.8)	0.6 (0.5)	6.6	-
12			H	Me	1.4 (0.5)	-0.7 (0.7)	-0.5 (0.3)	-0.4 (0.5)	-	-
13			H	Me	1.5 (0.4)	0.0 (0.2)	-1.0 (0.7)	0.0 (0.3)	-	-
14			H	Me	2.8 (0.7)	1.0 (0.3)	2.8 (1.6)	1.2 (0.5)	17	3.5
15			H	Me	-0.6 (0.1)	-0.3 (0.1)	0.2 (0.2)	-0.3 (0.1)	-	-
16			H	Me	-0.9 (0.1)	-0.3 (0.1)	0.3 (0.3)	0.1 (0.2)	-	-
17			H	Me	-0.2 (0.7)	0.0 (0.2)	-0.5 (0.7)	-0.9 (0.3)	-	-
18			H	Me	-0.5 (0.6)	0.0 (0.1)	-	-2.3 (0.5)	-	-
19		H	H	Me	-0.4 (0.2)	-0.4 (0.2)	0.8 (0.5)	-1.6 (0.3)	-	-
20		H	H	Me	3.3 (0.7)	5.3 (0.9)	5.1 (1.5)	0.2 (0.7)	9.3	6.3
21		H	H	Me	-0.6 (0.8)	1.0 (0.7)	-	-0.5 (0.4)	-	-
22		H	H	Me	1.4 (0.3)	2.5 (0.1)	-0.6 (0.7)	0.6 (0.3)	12	-
23					3.5 (0.2)	2.2 (0.4)	1.8 (1.0)	1.5 (0.4)	6.2	-
24					0.1 (0.1)	0.0 (0.1)	0.3 (0.3)	-0.3 (0.2)	-	-
27	H	H	OPr	Me	0.4 (0.2)	0.4 (0.1)	0.7 (0.1)	0.5 (0.3)	-	-
28		H	OPr	Me	-	2.7 (1.0)	-	-2.7 (1.2)	9.8	>50

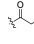



^aMedian value of the shift in the melting temperature. The total number of measurements for each compound and bromodomain was between 7 and 24. Ligand and protein concentrations were 100 and 2 μM, respectively. Standard errors of the mean are given in parentheses. The similar thermal shift values measured with the CREBBP bromodomain and its paralogue, EP300, are consistent with the fact that identical residues are present in the acetyllysine binding site of both proteins. ^b K_d values were determined by a competition binding assay^{55,56} in duplicate. Dose–response data and fitting curves can be found in the [Supporting Information](#). Dashes indicate data not acquired.

The affinity of the synthesized derivatives **39–50** for BAZ2B was assessed by an AlphaScreen competition binding assay at a compound concentration of 50 μM. Compound **47**, bearing an *o*-methyl and *m*-hydroxy substituent at the benzene ring, showed a 54% reduction in the magnitude of the signal relative to the negative control DMSO in the AlphaScreen binding assay, which translated into a K_D of 23 μM and a LE value of 0.27 kcal/mol per heavy atom. Upon substitution of the acetyl substituent at R₄ with a *m*-CF₃-benzoate group, an IC₅₀ value of 27 μM in the AlphaScreen assay and a K_D of 39 μM (BROMOscan) were measured for compound **50**.

Crystal structures of the most potent derivatives, **47** and **50**, in complex with BAZ2B were determined at 1.71 and 1.78 Å resolution, respectively. Compounds **47** and **50** (Figure 4A,B) have essentially identical binding modes in BAZ2B. As in the binding mode of hit **1b** in CREBBP (Figure 3), the *N*-acetyl substituent of the indole moiety of compounds **47** and **50** is engaged in hydrogen bonds with the side chain of the conserved Tyr1901 and Asn1944, where the hydrogen bond with Tyr1901 is bridged by a water molecule. An additional hydrogen bond is formed between the carbonyl group of the acetamide and the backbone NH of Asn1894 in the ZA loop.

Table 2. Evaluation of Compounds 39–50 Derived from 1g



Cmpd	R ₁	R ₂	R ₃	R ₄	K _d (μM) ^[a]	%Ctrl BAZ2B ^[b]
					BAZ2B	
1g	H	H	H		>50	91.3
39	H	CN	H	Acetyl	-	99.7
40	H	OMe	H	Acetyl	-	73.5
41	H	H	F	Acetyl	-	91.4
42	Me	H	OMe	Acetyl	-	71.9
43	OMe	H	H	Acetyl	-	86.3
44	H	H	OMe	Acetyl	-	89.6
45	Me	H	OMe		-	77.5
46	Me	H	OMe		140	87.3
47	Me	H	OH	Acetyl	23	54.2
48	OH	H	H	Acetyl	-	88.4
49	H	H	OH	Acetyl	-	86.3
50	Me	H	OH		39	29.8 (IC ₅₀ = 27 μM)

^aK_d values were determined by a competition binding assay^{55,56} in duplicate. Dose–response data and fitting curves are in the Supporting Information. ^bPercentage of the measured signal (i.e., percentage binding of acetylated histone peptide to BAZ2B) relative to the negative control at a compound concentration of 50 μM. Lower values indicate stronger binding of the compounds. The AlphaScreen competition binding assay was performed at Reaction Biology. Dashes indicate data not acquired.

The *o*-methyl substituent of the phenol ring provides sufficient steric hindrance to block the conformation of compounds 47 and 50 with their hydroxyphenyl ring pointing toward Trp1887, which is the first residue of the WPF segment in BAZ2B. The additional trifluoromethylbenzoate of compound 50 points toward the solvent (Figure 4B), which explains the similar affinity for BAZ2B of compounds 47 and 50 (Table 2).

As mentioned above, the bromodomains of BRD9 and BRPF1/3 belong to the same subfamily. Aiming to obtain further structural information, we took advantage of the availability in our laboratory of crystals of the apo state of the bromodomain of BRPF1b that were soaked in a solution of compound 1b. In this way, we determined the crystal structure of the complex of compound 1b with BRPF1b at a resolution of 1.35 Å (PDB entry 5D7X). Interestingly, the size of the so-called gatekeeper residue, small (Val1174 in CREBBP) and large (Phe714 in BRPF1b), has a noticeable influence on the orientation of the indole moiety (Figure 4C). Furthermore, the presence of the bulkier Phe714 residue in the BRPF1b bromodomain has a strong effect on the orientation of the dihydro-pyrazole ring that is rotated by ~180° in BRPF1b with respect to the complex with CREBBP. Despite these structural differences, compound 1b has a very similar affinity for the

bromodomains of CREBBP and BRPF1b with K_d values of 20 and 15 μM, respectively (see the Supporting Information).

The superposition of the X-ray structures of compound 1b in CREBBP and BRPF1b with compound 47 in BAZ2B provides additional evidence of the influence of the gatekeeper residue for ligand binding (Figure 4, D). Interestingly, the 6-membered ring of the indole moiety of compound 47 is located between the indole of compound 1b in BRPF1b and CREBBP because the gatekeeper residue in BAZ2B (Ile1950) is smaller than the one in BRPF1b (Phe714) and larger than that in CREBBP (Val1174). It is important to note that in these three crystal structures (viz., the 1b/CREBBP, 1b/BRPF1b, and 47/BAZ2B complexes) there are no crystal contacts in the binding site that could affect the orientation of the acetyl indole scaffold. Moreover, the structure of BAZ2B is essentially identical in the complex with compounds 47 and 50, and the same is observed for the structures of CREBBP in the complex with compound 1b and a previously reported acetyl benzene ligand (PDB entry 4TQN) that differ only by a small rigid-body displacement of the ZA loop. It is also interesting to compare with the orientation of the scaffold of the BAZ2B inhibitor 1a. The same progressive tilting of the indole emerges from the structural superposition of the complex of BAZ2B and the nanomolar inhibitor 1a (PDB entry 4RVR)⁴¹ with the crystal structures of the hit compound 1b in CREBBP and BRPF1b (Figure 4E). Overall, these structural data suggest that acetyl indole mimics the acetylated lysine side chain in its rather unselective binding to bromodomains. In addition, the precise orientation of the indole double-ring system and the substituent at its position 3 are influenced by the size of the gatekeeper residue that is different in different bromodomains.

CONCLUSIONS

We have discovered *in silico* a series of small-molecule antagonists of the bromodomains of CREBBP and BAZ2B by docking ~200 compounds containing an acetyl indole moiety, which we had identified by scaffold hopping from a potent BAZ2B ligand. Considering that only 14 compounds were tested *in vitro* (by a competition binding assay), the hit rates of the *in silico* screening based on scaffold hopping and docking are 50 and 29% for CREBBP and BAZ2B, respectively. One of the original hits (compound 1b) has equilibrium dissociation constants of 20, 15, and 5.3 μM for CREBBP, BRPF1b, and BRD9, respectively. With a relatively small derivatization campaign (i.e., ~30 derivatives), we were able to improve the affinity for CREBBP and BAZ2B and maintain the ligand efficiency (0.34 kcal/mol per heavy atom for both hit 1b and derivative 23 in CREBBP) or even slightly improve it (from <0.26 kcal/mol for hit 1g to 0.27 kcal/mol per heavy atom for compound 47 in BAZ2B). The crystal structures of three acetyl indole derivatives in complex with three different bromodomains confirm the binding mode predicted by docking with the acetyl oxygen of the ligand involved as a hydrogen bond acceptor in two hydrogen bonds with the conserved Asn side chain in the BC loop and a structural water that acts as bridge to the conserved Tyr of the ZA loop. Moreover, the X-ray structures show that the size of the gatekeeper side chain (Val1174, Ile1950, and Phe714 in the bromodomains of CREBBP, BAZ2B, and BRPF1b, respectively) influences the orientation of the indole moiety. This structural information can be used to further improve the selectivity for a single bromodomain target or a small subset of bromodomains sharing the same gatekeeper residue.

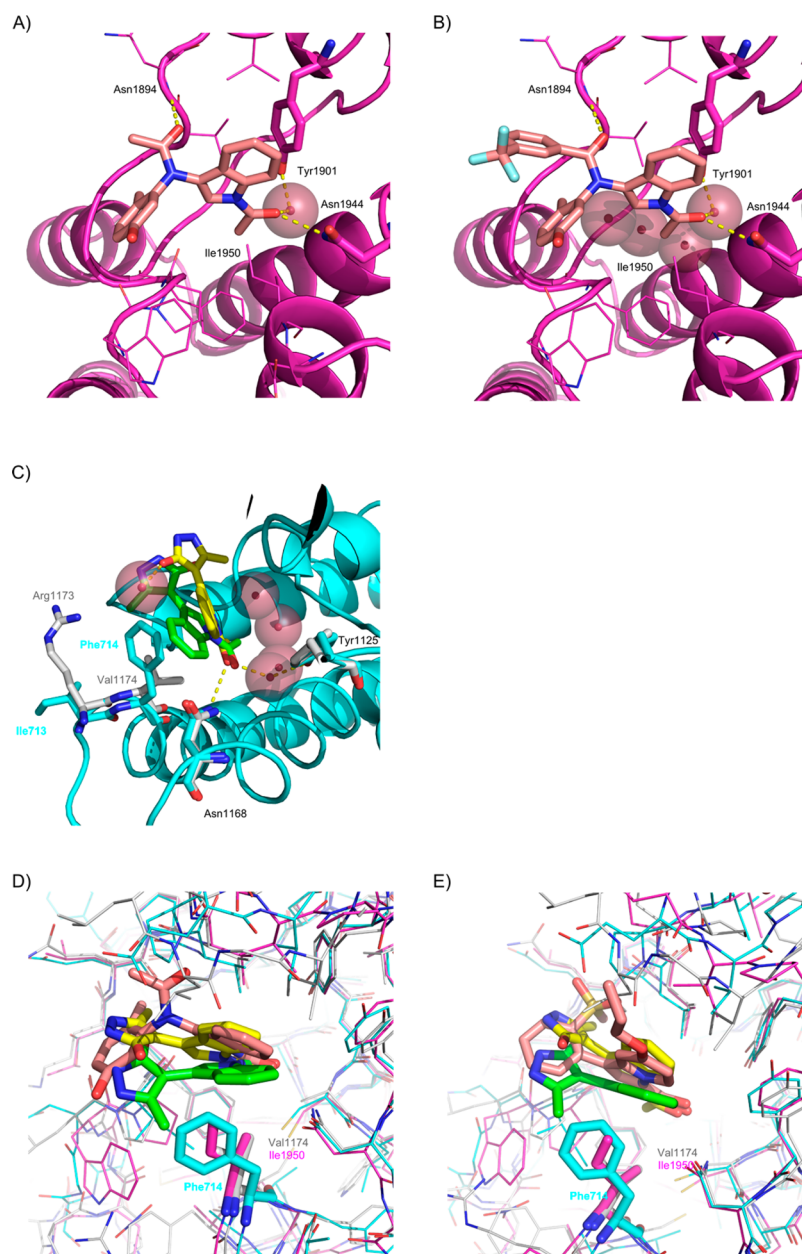


Figure 4. Crystal structures show the influence of the gatekeeper on the binding mode of the ligand. (A) Crystal structures of the BAZ2B bromodomain in complex with compound 47 (PDB entry 5E73). (B) Same as panel A for the complex with compound 50 (PDB entry 5E74). (C) Crystal structure of the complex of compound 1b (yellow) and the BRPF1b bromodomain (blue) (PDB entry 5D7X) structurally superposed to the crystal structure with CREBBP (compound 1b colored green and CREBBP side chains colored gray). (D) Superposition of the crystal structures of compound 47 (brown) in BAZ2B (pink) and compound 1b (green and yellow), in CREBBP (gray) and BRPF1b (blue). The side chain of the gatekeeper is shown as cylinders with labels for the residue number. (E) Same as panel D for the BAZ2B inhibitor 1a (brown) (PDB entry 4RVR). In all panels, hydrogen bonds are shown as yellow dashed lines and the crystallographic water molecules are represented by spheres.

EXPERIMENTAL SECTION

Scaffold Hopping. We have used an activity-oriented fingerprint that consists of (1) chemical features such as hybridization states and different types of hydrogen bonding donors and acceptors, (2) the two-dimensional topology index as a way to reflect the spatial arrangement of such features, and (3) three-dimensional shape descriptors (Figure S1 of the Supporting Information). A similarity coefficient is computed between two fingerprints ranging from 0 to 1, with 1 being the highest degree of similarity, where the two molecules are not necessarily identical. As such, scaffold hopping resembles pharmacophore mapping but distinguishes itself by using a molecular fingerprint.

Docking and Scoring. The genetic algorithm-based program for flexible ligand docking has been described in previous applications.^{50–52} Approximately 20 docking poses for each compound were first minimized by the CHARMM program⁵⁸ and subsequently ranked by a transferable scoring function.^{45,50–54}

Assays. Thermal shift measurements were taken as previously described.^{39,49} Thermal shift assays detect, by a fluorescent dye, the increase in the thermal stability of a protein in the presence of a ligand.⁵⁹ BROMOscan technology is a competition experiment that uses an immobilized ligand and a DNA-tagged bromodomain protein.^{55,56} Compounds that bind to the bromodomain of interest will prevent binding of the bromodomain to the immobilized ligand. The amount of bromodomain captured on the solid support is then quantified by qPCR, and dissociation constants are calculated.

AlphaScreen assays consist of a donor bead that is able to transfer singlet oxygen to an acceptor bead that is in the proximity, and as a result, the acceptor bead emits a luminescent/fluorescent signal. In the presence of a bromodomain ligand, the donor/acceptor complex is disrupted, leading to a loss of singlet oxygen transfer and loss of the fluorescent signal. Further details about the assays can be found in the [Supporting Information](#).

X-ray Crystallography. The His-tagged human bromodomains of CREBBP (residues 1081–1097), BRPF1b (residues 626–740), and BAZ2B (residues 1858–1972) were expressed in *Escherichia coli*. The purification procedures are reported in the [Supporting Information](#). The inhibitors were soaked into apo crystals of the bromodomains of BRPF1b and BAZ2B, while the structure of the complex of compound **1b** and CREBBP was obtained by cocrystallization as described in the [Supporting Information](#). Data collection and refinement statistics are listed in [Table S1](#).

■ ASSOCIATED CONTENT

Supporting Information

The Supporting Information is available free of charge on the [ACS Publications website](#) at DOI: [10.1021/acs.jmedchem.5b01757](https://doi.org/10.1021/acs.jmedchem.5b01757).

General procedures for scaffold hopping, synthesis and characterization, biophysical and biological evaluation of final compounds, and X-ray crystal structure refinement data ([PDF](#)) ([CSV](#))

Accession Codes

The PDB entries for CREBBP and BRPF1b in complex with the hit compound **1b** are 4TS8 and 5D7X, respectively. Coordinates and structure factors for the BAZ2B bromodomain in complex with compounds **47** and **50** have been deposited in the PDB as entries 5E73 and 5E74, respectively.

■ AUTHOR INFORMATION

Corresponding Authors

*E-mail: caflisch@bioc.uzh.ch. Phone: +41 44 635 55 21.

*E-mail: cristina.nevado@chem.uzh.ch. Phone: +41 44 635 39 45.

Notes

The authors declare no competing financial interest.

■ ACKNOWLEDGMENTS

We thank Dr. Emilie Frugier and Dr. Dimitrios Spiliotopoulos for interesting discussions and help with the thermal shift assay. We thank Lisa Cafilisch, Ursina Suter, and Cecilia Ferdenzi for protein purification and Dr. Alvaro Salvador and Anna Coppola for their efforts towards the synthesis of the hit compound **1b**. Nicholas Deerain is acknowledged for performing part of the thermal shift assays. We are grateful to the staff at PXI and PXIII beamlines, Swiss Light Source, Paul Scherrer Institute (Villigen, Switzerland), and at XDR1 beamline, ELETTRA Synchrotron Light Source (Trieste, Italy), for on-site assistance. This work was supported by the Swiss Cancer Society (Krebsliga, KFS-3098) and the Swiss National Science Foundation (315230_149897). We thank the Structural Genomics Consortium at University of Oxford for providing the plasmids of all the bromodomains but EP300 (provided by AddGene).

■ ABBREVIATIONS USED

BAZ2B, bromodomain adjacent to zinc finger domain 2B; BET, bromodomain and extra terminal domain; BRD2, -3, -4, -7, and

-9, bromodomain containing 2, 3, 4, 7, and 9, respectively; BRD4(1), first/second bromodomain of BRD4; BRPF1b, bromodomain and PHD finger containing 1; CBP, CREB binding protein; CREBBP, CREB binding protein; DMAP, 4-dimethylaminopyridine; DME, 1,2-dimethoxyethane; DMF, dimethylformamide; DMSO, dimethyl sulfoxide; EP300, E1A binding protein p300; HAT, histone acetyltransferase; LE, ligand efficiency; NMC, NUT midline carcinoma; NUT, nuclear protein in testis; PHD, plant homeodomain; PMB, 4-methoxybenzyl ether; SWI/SNF, switch/sucrose nonfermentable; TBAB, tetra-*n*-butylammonium bromide; TBAHS, tetrabutylammonium hydrogen sulfate; TBAI, tetrabutylammonium iodide

■ REFERENCES

- (1) Holliday, R. The inheritance of epigenetic defects. *Science* **1987**, *238*, 163–170.
- (2) Kouzarides, T. Chromatin modifications and their function. *Cell* **2007**, *128*, 693–705.
- (3) Flynn, E. M.; Huang, O. W.; Poy, F.; Oppikofer, M.; Bellon, S. F.; Tang, Y.; Cochran, A. G. A subset of human bromodomains recognizes butyryllysine and crotonyllysine histone peptide modifications. *Structure* **2015**, *23*, 1801–1814.
- (4) Prinjha, R. K.; Witherington, J.; Lee, K. Place your BETs: the therapeutic potential of bromodomains. *Trends Pharmacol. Sci.* **2012**, *33*, 146–153.
- (5) Müller, S.; Filippakopoulos, P.; Knapp, S. Bromodomains as therapeutic targets. *Expert Rev. Mol. Med.* **2011**, *13*, 1–21.
- (6) Hewings, D. S.; Rooney, T. P. C.; Jennings, L. E.; Hay, D. A.; Schofield, C. J.; Brennan, P. E.; Knapp, S.; Conway, S. J. Progress in the development and application of small molecule inhibitors of bromodomain-acetyl-lysine interactions. *J. Med. Chem.* **2012**, *55*, 9393–9413.
- (7) Filippakopoulos, P.; Knapp, S. Targeting bromodomains: epigenetic readers of lysine acetylation. *Nat. Rev. Drug Discovery* **2014**, *13*, 337–356.
- (8) Brand, M.; Measures, A. M.; Wilson, B. G.; Cortopassi, W. A.; Alexander, R.; Höss, M.; Hewings, D. S.; Rooney, T. P. C.; Paton, R. S.; Conway, S. J. Small molecule inhibitors of bromodomain-acetyl-lysine interactions. *ACS Chem. Biol.* **2015**, *10*, 22–39.
- (9) www.clinicaltrials.gov (accessed October 18, 2015).
- (10) Jennings, L. E.; Measures, A. R.; Wilson, B. G.; Conway, S. J. Phenotypic screening and fragment-based approaches to the discovery of small-molecule bromodomain ligands. *Future Med. Chem.* **2014**, *6*, 179–204.
- (11) Hay, D. A.; Fedorov, O.; Martin, S.; Singleton, D. C.; Tallant, C.; Wells, C.; Picaud, S.; Philpott, M.; Monteiro, O. P.; Rogers, C. M.; Conway, S. J.; Rooney, T. P. C.; Tumber, A.; Yapp, C.; Filippakopoulos, P.; Bunnage, M. E.; Müller, S.; Knapp, S.; Schofield, C. J.; Brennan, P. E. Discovery and optimization of small-molecule ligands for the CBP/p300 bromodomains. *J. Am. Chem. Soc.* **2014**, *136*, 9308–9319.
- (12) Ait-Si-Ali, S.; Poleskaya, A.; Filleur, S.; Ferreira, R.; Duquet, A.; Robin, P.; Vervish, A.; Trouche, D.; Cabon, F.; Harel-Bellan, A. CBP/p300 histone acetyl-transferase activity is important for the G1/S transition. *Oncogene* **2000**, *19*, 2430–2437.
- (13) Iyer, N. G.; Xian, J.; Chin, S. F.; Bannister, A. J.; Daigo, Y.; Aparicio, S.; Kouzarides, T.; Caldas, C. p300 is required for orderly G1/S transition in human cancer cells. *Oncogene* **2007**, *26*, 21–29.
- (14) Mujtaba, S.; He, Y.; Zeng, L.; Yan, S.; Plotnikova, O.; Sachchidanand; Sanchez, R.; Zeleznik-Le, N. J.; Ronai, Z.; Zhou, M. M. Structural mechanism of the bromodomain of the coactivator CBP in p53 transcriptional activation. *Mol. Cell* **2004**, *13*, 251–263.
- (15) Prives, C.; Hall, P. A. The p53 pathway. *J. Pathol.* **1999**, *187*, 112–126.

- (16) Coutts, A. S.; La Thangue, N. B. The p53 response: Emerging levels of co-factor complexity. *Biochem. Biophys. Res. Commun.* **2005**, *331*, 778–785.
- (17) Alarcon-Vargas, D.; Ronai, Z. p53-Mdm2 - the affair that never ends. *Carcinogenesis* **2002**, *23*, 541–547.
- (18) Wang, F.; Marshall, C. B.; Ikura, M. Transcriptional/epigenetic regulator CBP/p300 in tumorigenesis: structural and functional versatility in target recognition. *Cell. Mol. Life Sci.* **2013**, *70*, 3989–4008.
- (19) Lavau, C.; Du, C. C.; Thirman, M.; Zeleznik-Le, N. Chromatin-related properties of CBP fused to MLL generate a myelodysplastic-like syndrome that evolves into myeloid leukemia. *EMBO J.* **2000**, *19*, 4655–4664.
- (20) Pasqualucci, L.; Trifonov, V.; Fabbri, G.; Ma, J.; Rossi, D.; Chiarenza, A.; Wells, V. A.; Grunn, A.; Messina, M.; Elliot, O.; Chan, J.; Bhagat, G.; Chadburn, A.; Gaidano, G.; Mullighan, C. G.; Rabadan, R.; Dalla-Favera, R. Analysis of the coding genome of diffuse large B-cell lymphoma. *Nat. Genet.* **2011**, *43*, 830–837.
- (21) Bedford, D. C.; Brindle, P. K. Is histone acetylation the most important physiological function for CBP and p300? *Aging* **2012**, *4*, 247–255.
- (22) Hay, D. A.; Rogers, C. M.; Fedorov, O.; Tallant, C.; Martin, S.; Monteiro, O. P.; Müller, S.; Knapp, S.; Schofield, C. J.; Brennan, P. E. Design and synthesis of potent and selective inhibitors of BRD7 and BRD9 bromodomains. *MedChemComm* **2015**, *6*, 1381–1386.
- (23) Middeldjans, E.; Wan, X.; Jansen, P. W.; Sharma, V.; Stunnenberg, H. G.; Logie, C. SS18 Together with animal-specific factors defines human BAF-type SWI/SNF complexes. *PLoS One* **2012**, *7*, e33834.
- (24) Kaeser, M. D.; Aslanian, A.; Dong, M. Q.; Yates, J. R.; Emerson, B. M. BRD7, a Novel PBAF-specific SWI/SNF subunit, is required for target gene activation and repression in embryonic stem cells. *J. Biol. Chem.* **2008**, *283*, 32254–32263.
- (25) Tae, S.; Karkhanis, V.; Velasco, K.; Yaneva, M.; Erdjument-Bromage, H.; Tempst, P.; Sif, S. Bromodomain protein 7 interacts with PRMT5 and PRC2, and is involved in transcriptional repression of their target genes. *Nucleic Acids Res.* **2011**, *39*, 5424–5438.
- (26) Kang, J. U.; Koo, S. H.; Kwon, K. C.; Park, J. W.; Kim, J. M. Gain at chromosomal region 5p15.33, containing TERT, is the most frequent genetic event in early stages of non-small cell lung cancer. *Cancer Genet. Cytogenet.* **2008**, *182*, 1–11.
- (27) Scotto, L.; Narayan, G.; Nandula, S. V.; Subramaniam, S.; Kaufmann, A. M.; Wright, J. D.; Pothuri, B.; Mansukhani, M.; Schneider, A.; Arias-Pulido, H.; Murty, V. V. Integrative genomics analysis of chromosome 5p gain in cervical cancer reveals target over-expressed genes, including drosha. *Mol. Cancer* **2008**, *7*, 58.
- (28) Zhou, J.; Ma, J.; Zhang, B. C.; Li, X. L.; Shen, S. R.; Zhu, S. G.; Xiong, W.; Liu, H. Y.; Huang, H.; Zhou, M.; Li, G. Y. BRD7, a novel bromodomain gene, inhibits G1-S progression by transcriptionally regulating some important molecules involved in ras/MEK/ERK and Rb/E2F pathways. *J. Cell. Physiol.* **2004**, *200*, 89–98.
- (29) Wu, W. J.; Hu, K. S.; Chen, D. L.; Zeng, Z. L.; Luo, H. Y.; Wang, F.; Wang, D. S.; Wang, Z. Q.; He, F.; Xu, R. H. Prognostic relevance of BRD7 expression in colorectal carcinoma. *Eur. J. Clin. Invest.* **2013**, *43*, 131–140.
- (30) Park, Y. A.; Lee, J. W.; Kim, H. S.; Lee, Y. Y.; Kim, T. J.; Choi, C. H.; Choi, J. J.; Jeon, H. K.; Cho, Y. J.; Ryu, J. Y.; Kim, B. G.; Bae, D. S. Tumor suppressive effects of bromodomain-containing protein 7 (BRD7) in epithelial ovarian carcinoma. *Clin. Cancer Res.* **2014**, *20*, 565–575.
- (31) Burrows, A. E.; Smogorzewska, A.; Elledge, S. J. Polybromo-associated BRG1-associated factor components BRD7 and BAF180 are critical regulators of p53 required for induction of replicative senescence. *Proc. Natl. Acad. Sci. U. S. A.* **2010**, *107*, 14280–14285.
- (32) Drost, J.; Mantovani, F.; Tocco, F.; Elkon, R.; Comel, A.; Holstege, H.; Kerkhoven, R.; Jonkers, J.; Voorhoeve, P. M.; Agami, R.; Del Sal, G. BRD7 is a candidate tumour suppressor gene required for p53 function. *Nat. Cell Biol.* **2010**, *12*, 380–389.
- (33) Mantovani, F.; Drost, J.; Voorhoeve, P. M.; Del Sal, G.; Agami, R. Gene regulation and tumor suppression by the bromodomain-containing protein BRD7. *Cell Cycle* **2010**, *9*, 2777–2781.
- (34) Demont, E. H.; Bamborough, P.; Chung, C. W.; Craggs, P. D.; Fallon, D.; Gordon, L. J.; Grandi, P.; Hobbs, C. I.; Hussain, J.; Jones, E. J.; Le Gall, A.; Michon, A. M.; Mitchell, D. J.; Prinjha, R. K.; Roberts, A. D.; Sheppard, R. J.; Watson, R. J. 1,3-Dimethyl benzimidazolones are potent, selective inhibitors of the BRPF1 bromodomain. *ACS Med. Chem. Lett.* **2014**, *5*, 1190–1195.
- (35) Palmer, W. S.; Poncet-Montange, G.; Liu, G.; Petrocchi, A.; Reyna, N.; Subramanian, G.; Theroff, J.; Yau, A.; Kost-Alimova, M.; Bardenhagen, J. P.; Leo, E.; Shepard, H. E.; Tieu, T. N.; Shi, X.; Zhan, Y.; Zhao, S.; Barton, M. C.; Draetta, G.; Toniatti, C.; Jones, P.; Geck Do, M.; Andersen, J. N. Structure-guided design of IACS-9571, a selective high-affinity dual TRIM24-BRPF1 bromodomain inhibitor. *J. Med. Chem.* **2016**, *59*, 1440–1454.
- (36) Bennett, J.; Fedorov, O.; Tallant, C.; Monteiro, O.; Meier, J.; Gamble, V.; Savitsky, P.; Nunez-Alonso, G. A.; Haendler, B.; Rogers, C.; Brennan, P. E.; Müller, S.; Knapp, S. Discovery of a chemical tool inhibitor targeting the bromodomains of TRIM24 and BRPF. *J. Med. Chem.* **2016**, *59*, 1642–1647.
- (37) Ferguson, F. M.; Fedorov, O.; Chaikuad, A.; Philpott, M.; Muniz, J. R. C.; Felletar, I.; von Delft, F.; Heightman, T.; Knapp, S.; Abell, C.; Ciulli, A. Targeting low-druggability bromodomains: fragment based screening and inhibitor design against the BAZ2B bromodomain. *J. Med. Chem.* **2013**, *56*, 10183–10187.
- (38) Rooney, T. P. C.; Filippakopoulos, P.; Fedorov, O.; Picaud, S.; Cortopassi, W. A.; Hay, D. A.; Martin, S.; Tumber, A.; Rogers, C. M.; Philpott, M.; Wang, M. H.; Thompson, A. L.; Heightman, T. D.; Pryde, D. C.; Cook, A.; Paton, R. S.; Müller, S.; Knapp, S.; Brennan, P. E.; Conway, S. J. A series of potent CREBBP bromodomain ligands reveals an induced-fit pocket stabilized by a cation- π interaction. *Angew. Chem., Int. Ed.* **2014**, *53*, 6126–6130.
- (39) Unzue, A.; Xu, M.; Dong, J.; Wiedner, L.; Spiliotopoulos, D.; Cafilisch, A.; Nevado, C. Fragment-based design of selective nanomolar ligands of the CREBBP bromodomain. *J. Med. Chem.* **2016**, *59*, 1350–1356.
- (40) Drouin, L.; McGrath, S.; Vidler, L. R.; Chaikuad, A.; Monteiro, O.; Tallant, C.; Philpott, M.; Rogers, C.; Fedorov, O.; Liu, M. J.; Akhtar, W.; Hayes, A.; Raynaud, F.; Müller, S.; Knapp, S.; Hoelder, S. Structure enabled design of BAZ2-ICR, a chemical probe targeting the bromodomains of BAZ2A and BAZ2B. *J. Med. Chem.* **2015**, *58*, 2553–2559.
- (41) Chen, P.; Chaikuad, A.; Bamborough, P.; Bantscheff, M.; Bountra, C.; Chung, C.; Fedorov, O.; Grandi, P.; Jung, D.; Lesniak, R.; Lindon, M.; Müller, S.; Philpott, M.; Prinjha, R.; Rogers, C.; Selenski, C.; Tallant, C.; Werner, T.; Willson, T. M.; Knapp, S.; Drewry, D. H. Discovery and characterization of GSK2801, a selective chemical probe for the bromodomains BAZ2A and BAZ2B. *J. Med. Chem.* **2016**, *59*, 1410–1424.
- (42) Clark, P. G. K.; Vieira, L. C. C.; Tallant, C.; Fedorov, O.; Singleton, D. C.; Rogers, C. M.; Monteiro, O. P.; Bennett, J. M.; Baronio, R.; Müller, S.; Daniels, D. L.; Mendez, J.; Knapp, S.; Brennan, P. E.; Dixon, D. J. LP99: Discovery and synthesis of the first selective BRD7/9 bromodomain inhibitor. *Angew. Chem., Int. Ed.* **2015**, *54*, 6217–6221.
- (43) Theodoulou, N. H.; Bamborough, P.; Bannister, A. J.; Becher, I.; Bit, R. A.; Che, K. H.; Chung, C.-w.; Dittmann, A.; Drewes, G.; Drewry, D. H.; Gordon, L.; Grandi, P.; Leveridge, M.; Lindon, M.; Michon, A.-M.; Molnar, J.; Robson, S. C.; Tomkinson, N. C. O.; Kouzarides, T.; Prinjha, R. K.; Humphreys, P. G. Discovery of I-BRD9, a selective cell active chemical probe for bromodomain containing protein 9 inhibition. *J. Med. Chem.* **2016**, *59*, 1425–1439.
- (44) Kolb, P.; Kipouros, C. B.; Huang, D. Z.; Cafilisch, A. Structure-based tailoring of compound libraries for high-throughput screening: discovery of novel EphB4 kinase inhibitors. *Proteins: Struct., Funct., Genet.* **2008**, *73*, 11–18.
- (45) Zhao, H.; Huang, D. Hydrogen bonding penalty upon ligand binding. *PLoS One* **2011**, *6*, e19923.

(46) Unzue, A.; Lafleur, K.; Zhao, H.; Zhou, T.; Dong, J.; Kolb, P.; Liebl, J.; Zahler, S.; Caflich, A.; Nevado, C. Three stories on Eph kinase inhibitors: from in silico discovery to in vivo validation. *Eur. J. Med. Chem.* **2016**, *112*, 347–366.

(47) Unzue, A.; Dong, J.; Lafleur, K.; Zhao, H. T.; Frugier, E.; Caflich, A.; Nevado, C. Pyrrolo[3,2-b]quinoxaline derivatives as types I-1/2 and II Eph tyrosine kinase inhibitors: structure-based design, synthesis, and in vivo validation. *J. Med. Chem.* **2014**, *57*, 6834–6844.

(48) Lolli, G.; Caflich, A. High-throughput fragment docking into the BAZ2B bromodomain: efficient in silico screening for X-ray crystallography. *ACS Chem. Biol.* **2016**, *11*, 800–807.

(49) Xu, M.; Unzue, A.; Dong, J.; Spiliotopoulos, D.; Nevado, C.; Caflich, A. Discovery of CREBBP bromodomain inhibitors by high-throughput docking and hit optimization guided by molecular dynamics. *J. Med. Chem.* **2016**, *59*, 1340–1349.

(50) Zhao, H.; Caflich, A. Discovery of ZAP70 inhibitors by high-throughput docking into a conformation of its kinase domain generated by molecular dynamics. *Bioorg. Med. Chem. Lett.* **2013**, *23*, 5721–5726.

(51) Zhao, H.; Caflich, A. Discovery of dual ZAP70 and Syk kinases inhibitors by docking into a rare C-helix-out conformation of Syk. *Bioorg. Med. Chem. Lett.* **2014**, *24*, 1523–1527.

(52) Zhao, H.; Gartenmann, L.; Dong, J.; Spiliotopoulos, D.; Caflich, A. Discovery of BRD4 bromodomain inhibitors by fragment-based high-throughput docking. *Bioorg. Med. Chem. Lett.* **2014**, *24*, 2493–2496.

(53) Zhao, H.; Huang, D.; Caflich, A. Discovery of tyrosine kinase inhibitors by docking into an inactive kinase conformation generated by molecular dynamics. *ChemMedChem* **2012**, *7*, 1983–1990.

(54) Zhao, H. T.; Dong, J.; Lafleur, K.; Nevado, C.; Caflich, A. Discovery of a novel chemotype of tyrosine kinase inhibitors by fragment-based docking and molecular dynamics. *ACS Med. Chem. Lett.* **2012**, *3*, 834–838.

(55) Fabian, M. A.; Biggs, W. H.; Treiber, D. K.; Atteridge, C. E.; Azimioara, M. D.; Benedetti, M. G.; Carter, T. A.; Ciceri, P.; Edeen, P. T.; Floyd, M.; Ford, J. M.; Galvin, M.; Gerlach, J. L.; Grotzfeld, R. M.; Herrgard, S.; Insko, D. E.; Insko, M. A.; Lai, A. G.; Lelias, J. M.; Mehta, S. A.; Milanov, Z. V.; Velasco, A. M.; Wodicka, L. M.; Patel, H. K.; Zarrinkar, P. P.; Lockhart, D. J. A small molecule-kinase interaction map for clinical kinase inhibitors. *Nat. Biotechnol.* **2005**, *23*, 329–336.

(56) Quinn, E.; Wodicka, L.; Ciceri, P.; Pallares, G.; Pickle, E.; Torrey, A.; Floyd, M.; Hunt, J.; Treiber, D. Abstract 4238: BROMOscan - a high throughput, quantitative ligand binding platform identifies best-in-class bromodomain inhibitors from a screen of mature compounds targeting other protein classes. *Cancer Res.* **2013**, *73*, 4238.

(57) Vidler, L. R.; Brown, N.; Knapp, S.; Hoelder, S. Druggability analysis and structural classification of bromodomain acetyl-lysine binding sites. *J. Med. Chem.* **2012**, *55*, 7346–7359.

(58) Brooks, B. R.; Brooks, C. L., III; Mackerell, A. D., Jr; Nilsson, L.; Petrella, R. J.; Roux, B.; Won, Y.; Archontis, G.; Bartels, C.; Boresch, S.; Caflich, A.; Caves, L.; Cui, Q.; Dinner, A. R.; Feig, M.; Fischer, S.; Gao, J.; Hodoscek, M.; Im, W.; Kuczera, K.; Lazaridis, T.; Ma, J.; Ovchinnikov, V.; Paci, E.; Pastor, R. W.; Post, C. B.; Pu, J. Z.; Schaefer, M.; Tidor, B.; Venable, R. M.; Woodcock, H. L.; Wu, X.; Yang, W.; York, D. M.; Karplus, M. CHARMM: the biomolecular simulation program. *J. Comput. Chem.* **2009**, *30*, 1545–1614.

(59) Niesen, F. H.; Berglund, H.; Vedadi, M. The use of differential scanning fluorimetry to detect ligand interactions that promote protein stability. *Nat. Protoc.* **2007**, *2*, 2212–2221.